Available online at www.sciencedirect.com
SCIENCE DIRECT®
Journal of Power Sources 128 (2004) 263–269
JOURNAL OF POWER SOURCES
www.elsevier.com/locate/jpowsour

Lithium cobalt oxide cathode film prepared by rf sputtering

Cheng-Lung Liao, Kuan-Zong Fung*

Department of Materials Science and Engineering, National Cheng Kung University, Tainan 70101, Taiwan, ROC

Received 24 July 2003; accepted 30 September 2003

Abstract

Thin films of $LiCoO_2$ prepared by radio frequency magnetron sputtering on Pt-coated silicon are investigated under various deposited parameters such as working pressure, gas flow rate of Ar to O_2, and heat-treatment temperature. The as-deposited film was a nanocrystalline structure with (1 0 4) preferred orientation. After annealing at 500–700 °C, single-phase $LiCoO_2$ is obtained when the film is originally deposited under an oxygen partial pressure (P_{O_2}) from 5 to 10 mTorr. When the sputtering process is performed outside these P_{O_2} values, a second phase of Co_3O_4 is formed in addition to the HT-$LiCoO_2$ phase. The degree of crystallization of the $LiCoO_2$ films is strongly affected by the annealing temperature; a higher temperature enhances the crystallization of the deposited $LiCoO_2$ film. The grain sizes of $LiCoO_2$ films annealed at 500, 600 and 700 °C are about 60, 95, and 125 nm, respectively. Cyclic voltammograms display well-defined redox peaks. $LiCoO_2$ films deposited by rf sputtering are electrochemically active. The first discharge capacity of thin $LiCoO_2$ films annealed at 500, 600 and 700 °C is about 41.77, 50.62 and 61.16 μAh/(cm^2 μm), respectively. The corresponding 50th discharge capacities are 58.1, 72.2 and 74.9% of the first discharge capacity.

Keywords: Lithium cobalt oxide; Thin-film cathode; rf sputtering; Oxygen partial pressure; Lithium-ion battery

1. Introduction

Since the1980s, lithium-ion batteries have emerged as one of the most important power sources for portable electronics due to their high specific energy and good cycleability. In order to reduce weight for portable electronics, the demand for lighter and thinner batteries is increasing. To reduce the battery size, thin-film rechargeable batteries have received much attention. In lithium secondary batteries, $LiCoO_2$ has been widely used as the cathode material due to the advantages of high specific capacity, high operating voltage, and long cycle-life [1–5]. Crystalline $LiCoO_2$ has a layered structure with $R\bar{3}m$ symmetry in which the cobalt ions reside on the 3a sites of the octahedron, the lithium ions reside on the octahedral 3b interstices, and the oxygen anions form cubic close packing. This layered structure provides a 2D accessible path for Li-ion diffusion.

Thin films of $LiCoO_2$ can be obtained by various techmques such as radio frequency (rf) sputtering, pulsed laser deposition, spray pyrolysis, chemical vapour deposition, and reaction of cobalt metal [5–9]. In this work, the thin-film $LiCoO_2$ cathode is deposited on a Pt-coated silicon substrate by radio frequency magnetron sputtering using a $LiCoO_2$ target. Although the electrochemical properties and some fabrication parameters of rf-sputtered thin films of $LiCoO_2$ have been investigated [5–17], the effect of working pressure and Ar/O_2 ratio has not been thoroughly studied. Thus, the objective of this work is to determine the effect of working pressure, gas flow ratios of Ar to O_2, and annealing temperature on $LiCoO_2$ phase formation and crystallization, and on the electrochemical properties of a $LiCoO_2$ thin-film cathode that is deposited by the rf-sputtering technique.

2. Experimental

All the thin films of $LiCoO_2$ were grown by rf magnetron sputtering from a $LiCoO_2$ target with a 2 in. diameter. The $LiCoO_2$ target was sintered at 700 °C for 2 h by hot-pressing the $LiCoO_2$ powder, which was calcined from Li_2CO_3 (J.B.Baker, 99.6%), $CoCO_3$ (Alfa Aesar, 99%) at 700 °C for 12 h. Thin film deposition was carried out in the pressure range between 5 and 50 mTorr after pre-sputtering the target for 15 min. The total flow rate was set at 12 standard cubic centimeters per minute (sccm) with various ratios of Ar to O_2. The rf power was 100 W and the distance between the substrate and the target was 40 mm.

* Corresponding author. Tel.: +886-6-2380208; fax: +886-6-2380208.
E-mail address: kzfung@mail.ncku.edu.tw (K.-Z. Fung).

0378-7753/$ – see front matter © 2003 Elsevier B.V. All rights reserved.
doi:10.1016/j.jpowsour.2003.09.065

The substrate was a (1 0 0) silicon wafer which was covered with SiO_2 of 600 nm thickness. Pt layer of 200 nm served as a current-collector and a Ti layer of 20 nm was incorporated between the substrate and the pt current-collector in order to enhance adhesion at the interface between Pt and the SiO_2 substrate. The substrate was heated at 250 °C during the depostion process. In order to obtain the desired electrochemical properties, $LiCoO_2$ films were then annealed at 500–800 °C for 2 h in a controlled oxygen atmosphere to enhance the crystallization of the $LiCoO_2$ films.

The structure and the degree of crystallization of $LiCoO_2$ were characterized by X-ray diffraction using Cu Kα radiation (λ = 1.5418 Å), Raman spectroscopy (Coherent Innova 90), and transmission electron microscopy (JEOL, JEM-3010). The morphology and cross-section of the $LiCoO_2$ thin film were investigated by scanning electron microscopy (Philips, XL-40FEG). The contents of Li and Co in the films were analyzed by ICP-MS (Hewlett Packard 4500). Cyclic voltammetric (measured by EG&G, Potentiostat 273A) and charge–discharge characteristics (measured by Arbin, BT2043) of $LiCoO_2$ were also investigated for a Li|$LiCoO_2$ cell using a polycrystalline $LiCoO_2$ film as the cathode (active area = 1 cm^2), lithium metal as the anode, and 1 M $LiPF_6$ in propylene carbonate as the electrolyte.

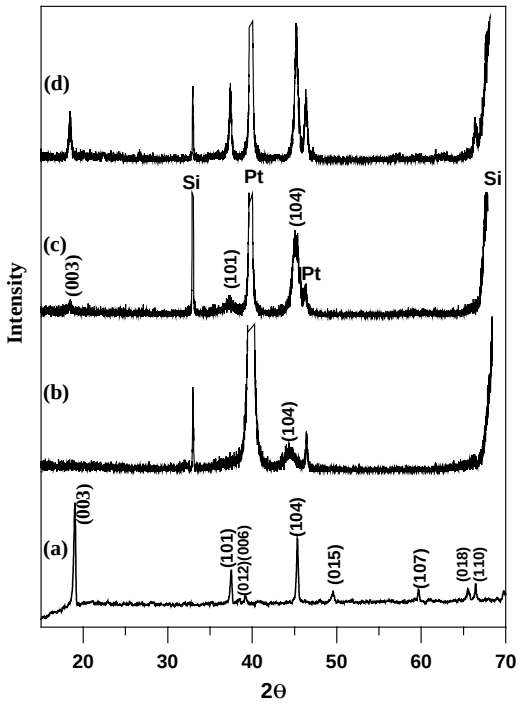

Fig. 1. XRD patterns of (a) $LiCoO_2$ powder, (b) as-deposited (substrate temperature was 250 °C), (c) 600 °C-annealed, and (d) 700 °C-annealed $LiCoO_2$ films.

3. Results and discussion

3.1. Structure characterization

It is known that $LiCoO_2$ exhibits three polymorphs, namely: hexagonal with $R\bar{3}m$ symmetry, cubic with $Fm3m$ symmetry, and spinel with $Fd3m$ symmetry [9]. HT-$LiCoO_2$ ($R\bar{3}m$) is usually employed as the cathode material in Li-ion batteries due to its good electrochemical properties [1–5]. The XRD pattern for $LiCoO_2$ powder synthesized at 700 °C is presented in Fig. 1(a). The pattern shows a random orientation of the HT-$LCoO_2$ structure with three major, well-defined reflections of (0 0 3), (1 0 4) and (1 0 1). The XRD pattern for a $LiCoO_2$ film that was deposited on a 250 °C-heated substrate is shown in Fig. 1(b). This pattern exhibits only a broad (1 0 4) reflection, showing that the film has a crystalline structure with (1 0 4) out-of-plane texture. This result is in contrast with published studies that have reported that amorphous $LiCoO_2$ films are obtained on deposition at ambient temperature by the rf sputtering technique [5,12–14]. On the other hand, Whitacre et al. [10] have found that preferred orientation can be grown at ambient temperature. It is believed that substrate heating provides energy for the rearrangement of lithium, cobalt, and oxygen atoms to form layered crystalline $LiCoO_2$ films. Therefore, the as-deposited films that have been grown at 250 °C and have shown (1 0 4) out-of-plane texture in this work are to be expected. In addition, the (104) reflection of the as-deposited $LiCoO_2$ film shown in Fig. 1(b) is broad and shifts to the lower 2θ position compared with that of $LiCoO_2$ powder shown in Fig. 1(a). This result suggests that the lithium, cobalt, and oxygen ions might not orderly occupy their ideal lattice positions in the layered structure. In other words, it appears that the as-deposited films do not have a well-crystallized structure.

The presence of the HT-$LiCoO_2$ phase is usually determined by a distinct separation of the (1 1 0) and (0 1 8) peaks or by the appearance of the (0 0 6) and (0 1 2) peaks in the XRD pattern. In this work, the as-deposited film displays only a broad (1 0 4) preferred orientation. It is difficult to verify the structure of the $LiCoO_2$ film by XRD analysis alone. Raman spectroscopy is a useful tool to distinguish between different symmetries in a given material. In sputtered $LiCoO_2$ films, different symmetries of $LiCoO_2$ will show different relative PS peaks in Raman spectra [18–21]. The Raman spectrum of an as-deposited $LiCoO_2$ films is shown if Fig. 2(a). There are two well-defined RS peaks at 468 and 582 cm^{-1}. These correspond to E_g and A_{1g} of the HT-$LiCoO_2$ structure. Further evidence of an as-deposited film with a crystalline structure is shown Fig. 2(b), which presents a typical TEM diffraction pattern of HT-$LiCoO_2$ with (0 0 3), (1 0 1), (1 0 4), and (1 1 0) reflections. From the combined results of XRD, TEM and Raman spectra, it is clear that an as-deposited crystalline HT-$LiCoO_2$ film with (1 0 4) preferred orientation is obtained when the film is grown on Pt-coated Si substrate.

It is well known that sputtered films exhibit a certain degree of texturing [22]. During the sputtering process, the deposited film may grow in a preferred orientation in order

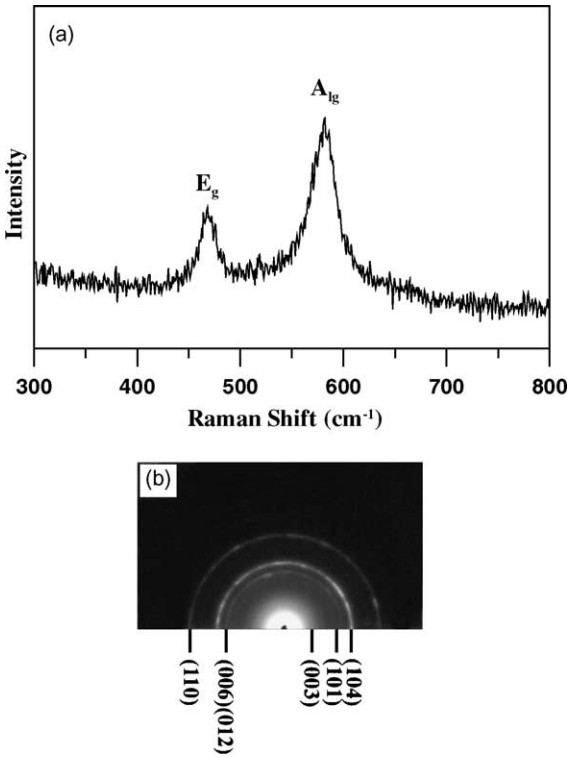

Fig. 2. (a) Raman spectrum and (b) TEM diffraction pattern of as-deposited $LiCoO_2$ film.

to minimize the volume strain energy or the surface energy. Furthermore, the volume strain energy is strongly affected by the thickness of deposited film. Based on the observations of Bates et al. [11], (1 0 1), (1 1 0) and (1 0 4) preferred orientation is favoured to minimize the volume strain energy when the thickness of the $LiCoO_2$ film is greater than 1 μm. Scanning electron micrographs reveal that the thickness of as-deposited and annealed $LiCoO_2$ film is greater than 1 μm (see Fig 3(c)–(h)). Thus, the (1 0 4) preferred orientation is due to strain relaxation of the film. From XRD analysis, only the diffraction of lattice planes oriented parallel to the substrate is detected. Therefore, this result indicates that the as-deposited film has a (1 0 4) plane parallel to the Pt-coated silicon substrate. The (1 0 4) preferred orientation is known to be helpful for lithium ions to intercalate into or de-intercalate from the layered $LiCoO_2$ structure [11].

3.2. Effect of heat treatment

It is well known that crystalline $LiCoO_2$ films exhibit better cycleability and specific energy than amorphous counterparts [1–5]. Therefore, heat treatment plays an important role in obtaining well-crystallized $LiCoO_2$ film. In order to increase the degree of crystallization of the $LiCoO_2$ films, the as-deposited $LiCoO_2$ films need to undergo a post-annealing at 500–800 °C. After film annealing at 600 °C, two more reflections of (1 1 0) and (0 0 3) are observed, as shown in Fig. 1(c). On increasing the annealing temperature to 700 °C, (0 0 3), (1 1 0) and (1 0 1) peaks are found to develop, as shown in Fig. 1(d). For films annealed at 750 and 800 °C, delamination occurs between the $LiCoO_2$ film and the substrated.

Electron micrographs of the sputtered $LiCoO_2$ films are shown in Fig 3(a)–(h). Top-view and cross-section images of the as-deposited $LiCoO_2$ film are presented in Fig. 3(a) and (e). The surface of the as-deposited film has a smooth morphology and the thickness is about 1.4 μm. The morphologies of crystalline $LiCoO_2$ films with grain sizes of about 60, 95 and 125 mm after annealing at 500, 600 and 700 °C for 2 h respectively are shown in Fig. 3(b)–(d). From the cross-section images shown in Fig. 3(f)–(h), the crystalline $LiCoO_2$ films exhibits a columnar structure that is perpendicular to the substrate. The thickness of the films annealed at 500, 600 and 700 °C is about 1.3, 1.3 and 1.2 μm, respectively.

From the XRD results, the as-deposited and annealed films are found to exhibit a HT-$LiCoO_2$ structure with (1 0 4) preferred orientation. Heat treatment at various temperatures enhances the crystallization of as-deposited $LiCoO_2$ films. Furthermore, SEM analysis shows that the grain size is enlarged and the thickness of the film is reduced with increasing annealing temperature. The increasing crystallization suggests that the lithium, cobalt and oxygen atoms rearrange to their ideal crystal positions after annealing. Moreover, shrinkage of the film indicates that all the ions are packed into a more close-packing arrangement after annealing.

3.3. Effect of working pressure

The Raman spectra of $LiCoO_2$ films deposited at different working pressures (5–50 mTorr) and then annealed at 600 °C for 2 h are presented in Fig. 4. The gas ratio of Ar to O_2 was fixed at 9:3. As described earlier, the RS peaks located at 487 and 597 cm^{-1} correspond to E_g and A_{1g} of layered $LiCoO_2$ [18–21]. On the other hand, the RS peaks at 521 and 690 cm^{-1} correspond to a Co_3O_4 second phase [20]. The results of Raman spectra indicate that the film deposited at 20 mTorr (P_{O_2} = 5 mTorr) and annealed at 600 °C for 2 h is composed of a single HT-$LiCoO_2$ phase. For films deposited under working pressures other than 20 mTorr (P_{O_2} = 5 mTorr), a Co_3O_4 second phase is obtained in addition to the HT-$LiCoO_2$ phase. For example, under working pressures of 5 mTorr (P_{O_2} = 1.25 mTorr) and 9 mTorr (P_{O_2} = 2.25 mTorr), dual phases of HT-$LiCoO_2$ and Co_3O_4 are observed. According to the crystal structure of $LiCoO_2$, it is clear that cobalt ion is in its trivalent state. By contrast, both divalent and trivalent cobalt ions are present in Co_3O_4. Due to the lower oxidation state of Co ions in Co_3O_4, the presence of Co_3O_4 can be attributed to a low oxygen partial pressure [23] when the working pressure is reduced to 5–9 mTorr The formation of Co_3O_4 is also observed when the working pressure is increased to 50 mTorr (P_{O_2} =

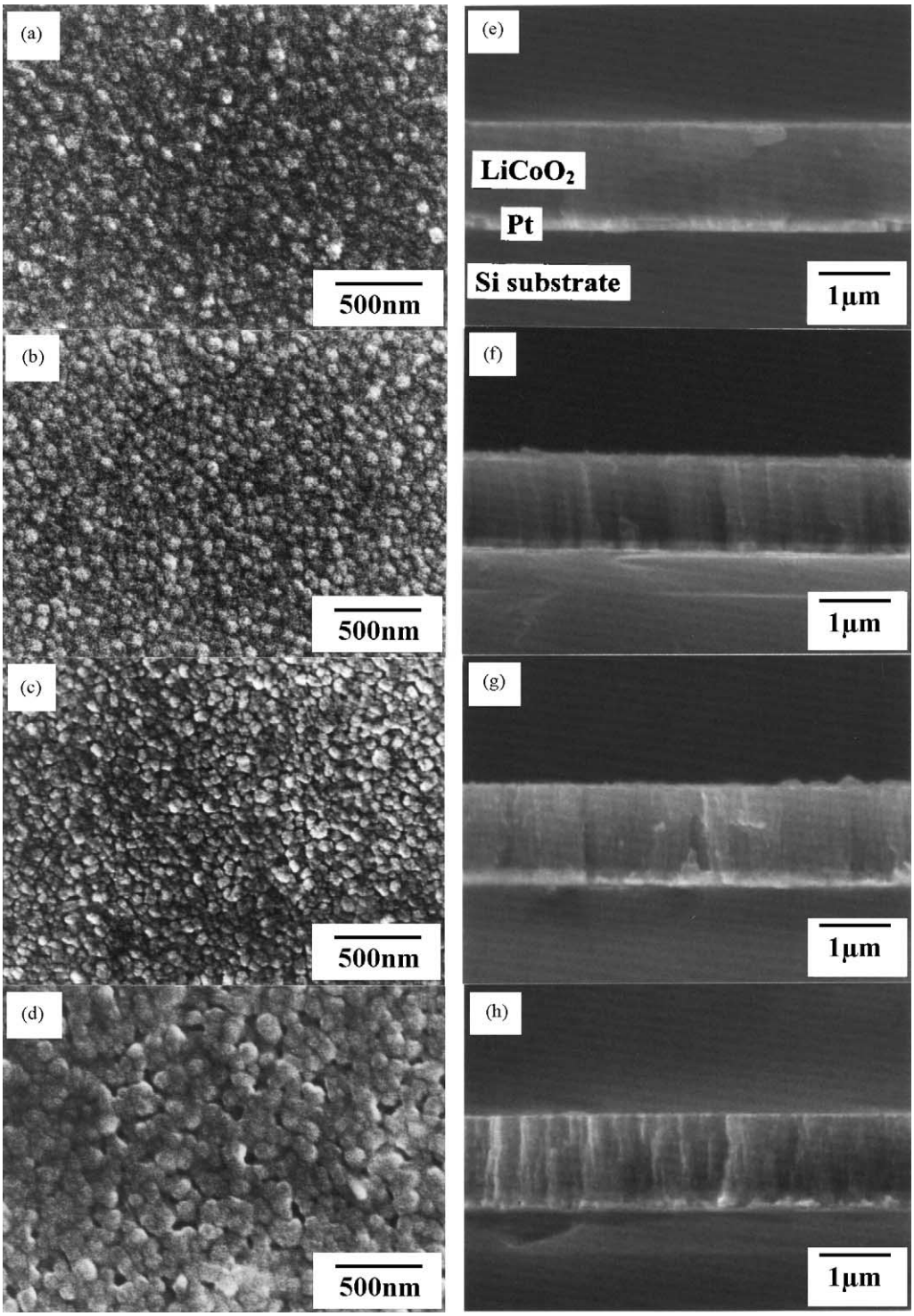

Fig. 3. SEM morphologies of (a) as-deposited, (b) 500 °C-annealed, (c) 600 °C-annealed, and (d) 700 °C-annealed $LiCoO_2$ films and cross-section images of (e) as-deposited, (f) 500 °C-annealed, (g) 600 °C-annealed, and (h)700 °C-annealed films.

1.25 mTorr). From ICP analysis, the Li:Co ratio is 1.02:1 and 0.91:1 for films grown under and $P_{O_2} = 5$ mTorr, 12.5 m Toor respectively. This suggests that the oxygen negative ions and the cobalt atoms that were sputtered from target by the accelerated Ar might re-sputter the film. Thus, the low atomic weight Li atoms on the substrate might be collided out of the substrate surface and result in a Li deficiency in the film. Therefore, in the higher oxygen partial pressure region, the formation of a Co_3O_4 phase is due to Li deficiency in the film.

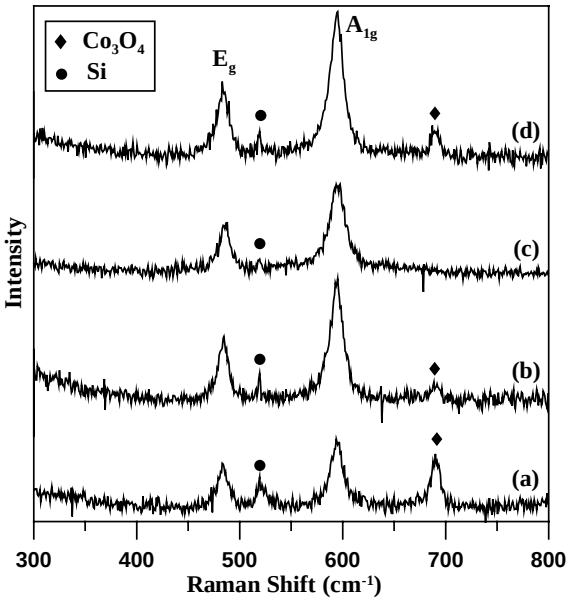

Fig. 4. Raman spectra of $LiCoO_2$ thin films obtained by rf sputtering at various working pressures: (a) 5 mTorr, (b) 9 mTorr, (c) 20 mTorr, (d) 50 mTorr and annealing at 600 °C for 2 h.

3.4. Effect of Ar to O_2 gas ratio

The Raman spectra of films deposited at various Ar:O_2 gas ratios and annealed at 600 °C for 2 h are shown in Fig. 5. The working pressure was fixed at 20 mTorr. In addition to the Raman band of layered $LiCoO_2$, there are two RS peaks that identified as the Co_3O_4 phase in Fig. 5(a) and (d).

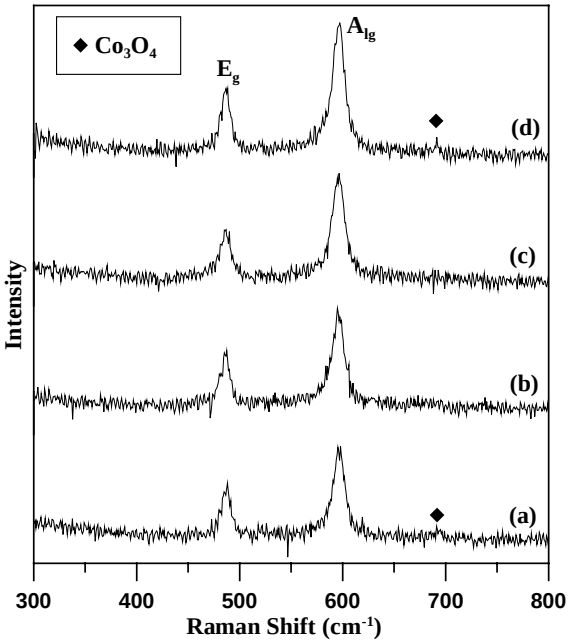

Fig. 5. Raman spectra of $LiCoO_2$ thin films deposited at sputtering gas flow rate of (a) Ar = 12 sccm, O_2 = 0 sccm, (b) Ar = 9 sccm, O_2 = 3 sccm, (c) Ar = 6 sccm, O_2 = 6 sccm, and (d) Ar = 3 sccm,O_2 = 9 sccm on Pt-coated silicon and annealed in O_2 at 600 °C for 2 h.

Variation of the Ar:O_2 ratio also affects the oxygen content in the deposition chamber. Similar to the effect on the working pressure, the presence of HT-$LiCoO_2$ and Co_3O_4 depends on the ratio of Ar to O_2. At a ratio of 12:0, Co_3O_4 is present in addition to $LiCoO_2$ due to the low oxygen partial pressure. For a sputtering gas with ratio of 9:3 and 6:6, a single $LiCoO_2$ phase is observed due to the adequate amount of oxygen available (P_{O_2} = 5 to 10 mTorr). When the ratio is changed to 3:9, a high oxygen partial pressure region is produced (P_{O_2} = 15 mTorr) and the formation of Co_3O_4 can be attributed to a deficiency that results from re-sputtering in the thin-film deposition process.

The ratio of Ar to O_2 also affects the thickness of $LiCoO_2$ films. The deposition rates have been found to vary roughly linearly with the ratio of Ar to O_2 [10]. $LiCoO_2$ films grown at high ratio of Ar to O_2 have a thicker thickness than these grown at lower ratios. This is because the amount of Ar gas enhances the sputtering efficiency to obtain thicker films.

3.5. Electrochemica1 studies

The cyclic voltammogram for a 700 °C-annealed $LiCoO_2$ film is shown in Fig. 6. Three sets of redox peaks that correspond to three plateau in the charge–discharge curve (shown in Fig. 7(a)) are observed. The anodic peak (a) located at 3.95 V, the cathodic peak (a′) located at 3.86 V, the peaks b–b′ located at about 4.07 V and the peaks c–c′ located at about 4.16 V are in good agreement with those previously reported [24,25]. The largest peaks (a–a′) correspond to the main de-intercalation/intercalation reactions of Li ions from/into the layered structure. The other two small sets of peaks correspond to phase transitions between ordered and disordered Li-ion arrangements in the CoO_2 framework [25]. The fact that the anodic peak (a) is larger than the cathodic peak (a′) in the first charge–discharge cycle suggests that the reaction is not completely reversible.

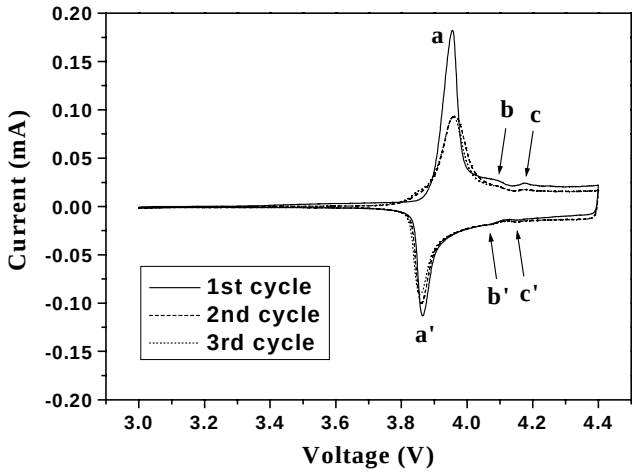

Fig. 6. Cyclic voltammogram of 700 °C-annealed $LiCoO_2$ cell with $LiPF_6$ electrolyte at a sweep rate of 0.1 mV/s.

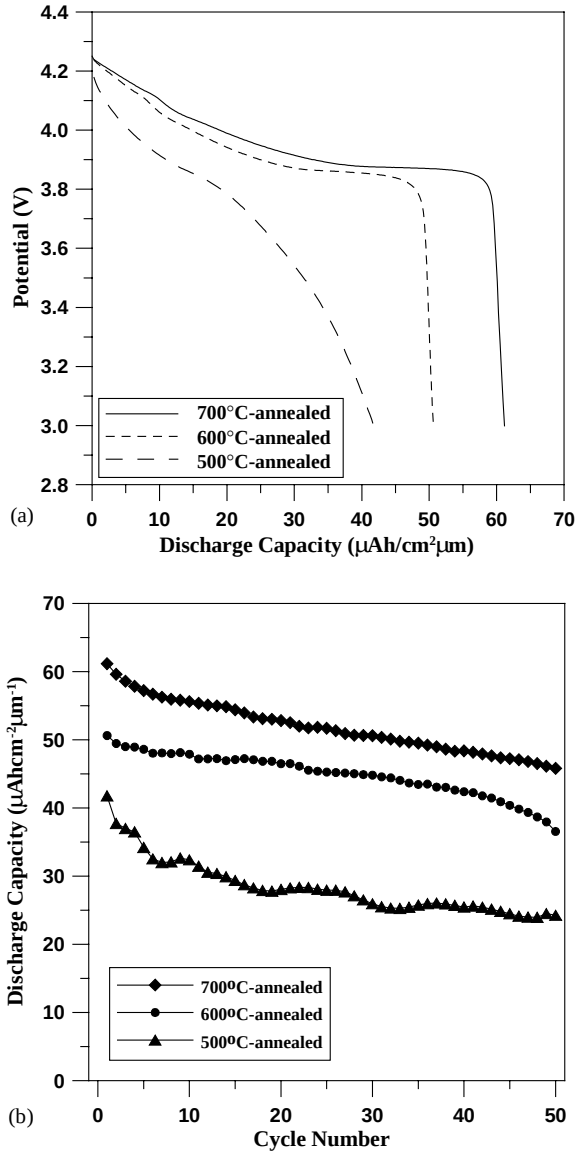

Fig. 7. (a) Discharge curves for Li|$LiCoO_2$ cell with $LiCoO_2$ films annealed in O_2 atmosphere at 500, 600 and 700 °C for 2 h, (b) discharge capacity vs. cycle number of 500, 600 and 700 °C-annealed films.

Discharge curves for a Li|$LiCoO_2$ cell using deposited $LiCoO_2$ films are given in Fig. 7(a). These cells were assembled using $LiCoO_2$ films that were annealed at 500, 600 and 700 °C for 2 h, respectively. Electrochemical measurements were carried out at a discharge rate of 10 μA/cm^2 in the potential range 4.25–3.0 V. For the cell with a 700 °C-annealed film, the open-circuit voltage (OCV) is 4.24 V. After discharging, the voltage decreases gradually and then reaches a plateau near 3.9 V. This plateau is consistent with the CV result. After a capacity of 58.35 μAh/(cm^2 μm) is discharged, the voltage drops rapidly. After reaching the cut-off voltage of 3.0 V, the total capacity discharged is found to be 61.16 μAh/(cm^2 μm).

For the cell with a 600 °C-annealed film, the OCV is 4.24 V. Such a high voltage indicates that an electrochemically active $LiCoO_2$ phase is also formed. The voltage drops noticeably as the discharge continues. A 3.9 V plateau is observed when the cell is discharged from 20 to 49 μAh/(cm^2 μm). After the short plateau, the voltage decreases gradually. The total discharged capacity is 50.62 μAh/(cm^2 μm) which is much less then that for the cell with a 700 °C-annealed cathode film. These results suggest that the annealing process is crucial for obtaining electrochemically active $LiCoO_2$ with a well-crystallized layered structure. When the film is annealed at 700 °C, the high temperature enhances the mobility of ions and results in a greater extent of electrochemically active $LiCoO_2$ film. Thus, a well-defined plateau is observed and a higher capacity is obtained. When the film is annealed at 500 °C, the layered $LiCoO_2$ is not well-crystallized. Therefore, the 3.9 V plateau is not clearly observed and the capacity is only 41.77 μAh/(cm^2 μm).

The cell discharge capacity with respect to cycle number is shown in Fig. 7(b). Because the extent of crystallization of $LiCoO_2$ film can be enhanced by a higher annealing temperature, the discharge capacity increases with increase in the annealing temperature. After long-term charge–discharge tests, the capacity of a 700 °C-annealed film decreases slowly. Compared with the initial discharge capacity, the capacity loss is 25.l, 27.8 and 41.9% for the 700, 600 and 500 °C-annealed films after 50 cycles, respectively. The capacity fading of $LiCoO_2$ films becomes worse when the film is annealed at a lower temperature. When the as-deposited film is annealed at a lower temperature, it is reasonable to expect that the film might not completely crystallize in a layered structure. Thus, some lithium ions may not be able to migrate to the desired lattice sites during the intercalation process. As a result, the amount of electrochemically active lithium ions gradually decreases on cycling. In a well-structured $LiCoO_2$ film, most lithium ions can intercalate repeatedly into the lithium layer of the rhombohedral lattice. Therefore, capacity fading is less noticeable in the 700 °C annealed $LiCoO_2$ film.

4. Conclusions

A nanocrystalline HT-$LiCoO_2$ film is obtained when the film is deposited on a 250 °C-heated Si substrate under a P_{O_2} that ranges from 5 to 10 mTorr. Both the as-deposited and annealed films exhibit (1 0 4) preferred orientation. When films are deposited at a P_{O_2} higher than 10 mTorr or lower than 5 mTorr, a Co_3O_4 second phase is obtained in addition to the $LiCoO_2$ phase. Therefore, the oxygen partial pressure plays an important role in the phase formation of the sputtered $LiCoO_2$ films. The degree of crystallization and the electrochemical properties of the $LiCoO_2$ films are enhanced by increasing the annealing temperature from 500 to 700 °C. The grain sizes of the films are about 60, 95 and 125 nm after annealing at 500, 600 and 700 °C for 2 h, respectively. The discharge capacity is about 41.77, 50.62

and 61.16 μAh/(cm^2 μm) for 500, 600 and 700 °C-annealed films, respectively. Furthermore, the corresponding 50th discharge capacities are 58.1, 72.2 and 74.9% of the first discharge capacity.

Acknowledgements

This work was supported by NHRI, Taiwan under the contract #NHRI-EX90-8924EL.

References

[1] K. Mizushima, P.C. Jones, P.C. Wiseman, J.B. Goodenough, Mater. Res. Bull. 15 (1980) 783.
[2] T. Nagaura, K. Tozawa, Progr. Batt. Solar Cells 9 (1991) 209.
[3] M. Antaya, J.R. Dahn, J.S. Preston, E. Rossen, J.N. Reimers, J. Electrochem. Soc. 140 (1993) 575.
[4] P. Fragnaud, T. Brousse, D.M. Schleich, J. Power Sources 63 (1996) 187.
[5] B. Wang, J.B. Bates, F.X. Hart, B.C. Sales, R.A. Zuhr, J.D. Robertson, J. Electrochem. Soc. 143 (1996) 3203.
[6] A. Antaya, J.R. Dahn, J.S. Preston, E. Rossen, J.N. Reimers, J. Electrochem. Soc. 140 (1993) 575.
[7] S.J. Lee, J.K. Lee, D.W. Kim, H.K. Baik, J. Electrochem. Soc. 143 (1996) L268.
[8] K.A. Striebel, C.Z. Deng, S.J. Wen, E.J. Cairns, J. Electrochem. Soc. 143 (1996) 1821.
[9] Seung-Wan Song, Kyoo-Seung Han, and Masahiro Yoshimura, J. Am. Ceram. Soc. 83 (2000) 2839.
[10] J.F. Whitacre, W.C. West, E. Brandon, B.V. Ratnakumar, J. Electrochem. Soc. 148 (2001) A1078.
[11] J.B. Bates, N.J. Dudney, B.J. Neudecker, F.X. Hart, H.P. Jun, S.A. Hackney, J. Electrochem. Soc. 147 (2000) 59.
[12] R.B. Goldner, P. Zerigian, T.Y. Liu, N. Clay, F. Vereda, T.E. Haas, Solid State Ionics 548 (1999) 131.
[13] P. Fragnaud, T. Brousse, D.M. Schleich, J. Power Sources 63 (1996) 187.
[14] C.N. Polo Da Fonseca, J. Davalos, M. Kleinke, M.C.A. Fantini, A. Gorenstein, J. Power Sources 81-82 (1999) 575.
[15] P.J. Bouwman, B.A. Boukamp, H.J.M. Bouwmeester, H.J. Wondergem, P.H.L. Notten, J. Electrochem. Soc. 148 (2001) A311.
[16] J.F. Whitacre, W.C. West, B.V. Ratnakumar, J. Power Sources 103 (2001) 134.
[17] L.-K. Lee, S.-J. Lee, H.-K. Baik, H.-Y. Lee, S.-W. Jang, S.-M. Lee, Electrochem. Solid-State Lett. 2 (1999) 512.
[18] W. Huang, R. Frech, Solid State Ionics 86-88 (1996) 395.
[19] M. Inaba, Y. Iriyama, Z. Ogumi, Y. Todzuka, A. Tasaka, J. Raman Spectrosc. 28 (1997) 613.
[20] J.D. Perkins, M.L. Fu, D.M. Trickett, J.M. McGraw, T.F. Ciszek, P.A. Parilla, C.T. Rogers, D.S. Ginley, Mater. Res. Soc. Symo. Proc. 496 (1998) 329.
[21] J.D. Perkins, C.S. Balm, P.A. Parilla, J.M. McGraw, M.L. Fu, M. Duncan, H. Yu, D.S. Ginley, J. Power Sources 81-82 (1999) 675.
[22] P. Sigmund, Phys. Rev. 184 (1969) 383.
[23] J.D. Perkins, C.S. Bahn, J.M. McGraw, P.A. Parilla, D.S. Ginley, J. Electrochem. Soc. 148 (2001) A1302.
[24] Isamu Uchida and Hajime Sato, J. Electrochem. Soc. 142 (1995) L139.
[25] J.N. Reimers, J.R. Dalin, J. Electrochem. Soc. 139 (1992) 2091.